Time Domain Parabolic Equation Method for Scattering Analysis of Electrically Large Coated Objects by using Impedance Boundary Condition

Ling Guan and Shifei Tao

School of Electronic and Optical Engineering
Nanjing University of Science and Technology, Nanjing, Jiangsu Province 210094, China
s.tao@njust.edu.cn

Abstract ─ The time domain parabolic equation method (TDPE) is an efficient tool for analyzing electromagnetic (EM) scattering by electrically large objects. It reduces the cost of computational resources by dividing three-dimensional solution space into multiple two-dimensional transverse planes for calculating scattered fields one by one. For thin coated perfectly electrically conducting (PEC) objects, the efficiency of TDPE method will decrease if dielectric is considered to be meshed. As an approximate method, Leontovich impedance boundary condition (IBC) handles this problem by modeling a surface impedance on the outer surface of coating dielectric, instead of solving Maxwell's equations in the dielectric domain. Thus in this paper, TDPE method based on Leontovich IBC is proposed to analyze broadband scattering problems of large-scale coated PEC objects. Numerical results have validated the accuracy and efficiency of the proposed method.

Index Terms ─ Coated objects, impedance boundary condition, time domain parabolic equation, wideband electromagnetic scattering.

I. INTRODUCTION

Recently, accurate and efficient prediction of wide-band electromagnetic (EM) scattering characteristic for electrically large objects has been required increasingly in many regions, because the broadband detection and stealth of targets are applied widely. The radar cross sections (RCS) evaluation of objects is a vital tool for the target identification and the optimization of objects' shape or coating. However, the coated material for stealth and camouflage will increase the complexity and reduce the efficiency in the EM scattering analysis. Therefore, it is necessary to develop an accurate and efficient numerical method to handle this problem. The parabolic equation (PE) method has been widely used to analyze the propagation of acoustic wave [1,2], light wave [3,4] and seismic wave [5], because it modules the wave propagating along the paraxial direction. The method is firstly proposed by Lenontovich and Fock in [6], where the electromagnetic (EM) wave diffraction on the earth's surface is researched. After then, the EM wave propagation over obstacle surface [7], irregular terrain [8] and even expressway [9] is also modeled, calculated and analyzed. The PE method converts a three-dimensional (3D) problem to multiple two-dimensional (2D) problems by marching the solving plane. In this way, the computational resources can be reduced dramatically [10-13]. Recently, more attention is focused on the solution in time domain since the requirement for broadband or transient analysis becomes more urgent [14]. The 2D time domain parabolic equation (TDPE) developed by Murphy is utilized to analyze ocean acoustic propagation [16]. Later, a 3D vector TDPE is proposed for solving wide-band EM scattering problems of perfectly conducting (PEC) objects with high efficiency [17].

However, less work reports on the wide-band analysis of composite objects, especially for coated objects [18,19]. In traditional rigorous methods, e.g., surface integral equation (SIE) [20-24] and volume-surface integral equation (VSIE) [25], the number of unknowns will increase significantly if coating dielectric is meshed because thickness is usually small compared to the wavelength. Leontovich impedance boundary condition (IBC) which prescribes on the outer surface of coating materials can overcome this problem [26]. It avoids the dense grids and costly solution inside the coating by constituting a local relationship between the tangential components of the electric field and magnetic field. In [27], IBC is introduced into time-domain integral equation (TDIE) to analyze transient scattering from coated bodies. Both unknown electric and magnetic currents are considered and modeled independently to guarantee the continuity of normal components across mesh edges. The method is free of spurious resonant solutions and exact fields can be obtained. TDIE presents obvious advantages when analyzing open boundary problems of homogeneous scatterers because it automatically satisfies the radiation condition. Only scatterers need a discretization rather than the whole solution space. This results in a sharp decrease on the number of unknowns. However, huge

Submitted On: May 19, 2018
Accepted On: September 24, 2018

1054-4887 © ACES

computational resources will be cost on solving dense matrix equations in TDIE, even if it is accelerated by the plane-wave time-domain algorithm and multilevel fast multipole algorithm which restricts its application on analyzing large-scale scattering and radiation problems.

In this paper, we propose TDPE with Leontovich IBC to solve wide-band EM scattering from coated objects. The dielectric region is described by IBC, which leads to a great reduction in computing times and memory requirements. The implicit finite difference (FD) scheme of Crank–Nicolson (CN) type is employed to solve the parabolic equation. The transient scattered fields can be computed plane by plane along the forward wave propagation direction. Additionally, the complete scattering field in all directions can be obtained by the rotating TDPE method.

II. THREE-DIMENSIONAL TIME DOMAIN PARABOLIC EQUATION METHOD

A. Vector three-dimensional TDPE formulations

Parabolic equation is an approximate form of the wave equation in paraxial direction. The wave equation in source-free region can be written as:

$$\frac{\partial^2\psi}{\partial x^2}+\frac{\partial^2\psi}{\partial y^2}+\frac{\partial^2\psi}{\partial z^2}+k^2\psi=0, \tag{1}$$

where ψ denotes the scattered field component and k is the wave number.

Assuming the x axis is the paraxial direction of the parabolic equation, the reduced scattered field can be defined as:

$$u(x,y,z)=e^{-ikx}\psi(x,y,z). \tag{2}$$

Substitute (2) to (1) and factorize it, the forward and backward parabolic equation can be obtained:

$$\begin{cases}\dfrac{\partial u_+}{\partial x}=-ik\left(1-\sqrt{Q}\right)u_+\\ \dfrac{\partial u_-}{\partial x}=-ik\left(1+\sqrt{Q}\right)u_-\end{cases}, \tag{3}$$

where $Q=\dfrac{1}{k^2}\left(\dfrac{\partial^2}{\partial y^2}+\dfrac{\partial^2}{\partial z^2}\right)+n^2$ denotes the pseudo differential operator. u_+ and u_- represent the forward and backward components of the reduced scattered field.

With the first order Taylor series expansion, Q can be approximated as:

$$\sqrt{Q}\approx 1+\frac{Q-1}{2}. \tag{4}$$

Thus, the standard parabolic equation can be obtained:

$$\frac{\partial u}{\partial x}=\frac{i}{2k}\left(\frac{\partial^2}{\partial y^2}+\frac{\partial^2}{\partial z^2}\right)u. \tag{5}$$

The vector PE is composed of three scalar parabolic equations in three dimensions. The standard vector PE in free space can be written as:

$$\begin{cases}\dfrac{\partial^2 u_x}{\partial y^2}+\dfrac{\partial^2 u_x}{\partial z^2}+2ik\dfrac{\partial u_x}{\partial x}=0\\ \dfrac{\partial^2 u_y}{\partial y^2}+\dfrac{\partial^2 u_y}{\partial z^2}+2ik\dfrac{\partial u_y}{\partial x}=0\\ \dfrac{\partial^2 u_z}{\partial y^2}+\dfrac{\partial^2 u_z}{\partial z^2}+2ik\dfrac{\partial u_z}{\partial x}=0\end{cases}. \tag{6}$$

Define a Fourier transform as:

$$\prod(x,y,z,s)=\frac{1}{2\pi}\int_{-\infty}^{\infty}\tilde{F}(k)u(x,y,z,k)e^{-iks}dk, \tag{7}$$

where $\tilde{F}(k)=\int_0^\infty \boldsymbol{E}^i e^{i\omega t}dt$ is a spectrum function, $\boldsymbol{E}^i$ represents the incident plane wave, $s=ct-x$ is the distance from the paraxial wave-front ct and c is the light speed.

Using the Fourier transform in (7), the three dimensional vector PE in time domain is obtained:

$$\frac{\partial^2\prod_\xi}{\partial y^2}+\frac{\partial^2\prod_\xi}{\partial z^2}-2\frac{\partial^2\prod_\xi}{\partial x\partial s}=0 \qquad \xi=x,y,z, \tag{8}$$

where $\prod_\xi$ $(\xi=x,y,z)$ denotes the components of transient reduced scattered field for x–, y– and z– directions, respectively.

Applying central difference scheme to (8), the semi-discretized form of the time-domain PE can be derived:

$$\begin{aligned}&\frac{8}{\Delta x\Delta s}\left(\begin{matrix}\prod_{\xi,l+1}^{m+1}-\prod_{\xi,l+1}^{m}\\ -\prod_{\xi,l}^{m+1}+\prod_{\xi,l}^{m}\end{matrix}\right)=\\ &\qquad\frac{1}{\Delta z^2}\nabla_z^2\left(\begin{matrix}\prod_{\xi,l+1}^{m+1}+\prod_{\xi,l+1}^{m}\\ +\prod_{\xi,l}^{m+1}+\prod_{\xi,l}^{m}\end{matrix}\right)+\frac{1}{\Delta y^2}\nabla_y^2\left(\begin{matrix}\prod_{\xi,l+1}^{m+1}+\prod_{\xi,l+1}^{m}\\ +\prod_{\xi,m+1,l}+\prod_{\xi,m,l}\end{matrix}\right),\\ &\qquad\qquad\qquad\qquad\qquad\qquad\qquad\qquad\qquad\qquad\xi=x,y,z\end{aligned} \tag{9}$$

in which $\prod_{\xi,l}^{m}$ $(\xi=x,y,z)$ is the unknown, Δx, Δy, Δz are the spatial range steps in three dimensions and Δs is the time step. ∇_y^2 and ∇_z^2 denote the second-order difference operator along the y-and z-axes, respectively:

$$\begin{aligned}&-\frac{1}{\Delta z^2}\prod_{\xi,l+1}^{m+1,p,q-1}-\frac{1}{\Delta y^2}\prod_{\xi,l+1}^{m+1,p-1,q}-\frac{1}{\Delta z^2}\prod_{\xi,l+1}^{m+1,p,q+1}-\frac{1}{\Delta y^2}\prod_{\xi,l+1}^{m+1,p+1,q}+\left(\frac{8}{\Delta x\Delta s}+\frac{2}{\Delta z^2}+\frac{2}{\Delta y^2}\right)\prod_{\xi,l+1}^{m+1,p,q}\\ &=\frac{1}{\Delta y^2}\prod_{\xi,l+1}^{m,p-1,q}+\frac{1}{\Delta z^2}\prod_{\xi,l+1}^{m,p,q-1}+\frac{1}{\Delta y^2}\prod_{\xi,l+1}^{m,p+1,q}+\frac{1}{\Delta z^2}\prod_{\xi,l+1}^{m,p,q+1}+\frac{1}{\Delta y^2}\prod_{\xi,l}^{m+1,p-1,q}+\frac{1}{\Delta z^2}\prod_{\xi,l}^{m,p,q+1}+\left(\frac{8}{\Delta x\Delta s}-\frac{2}{\Delta z^2}-\frac{2}{\Delta y^2}\right)\prod_{\xi,l+1}^{m,p,q}+\left(\frac{8}{\Delta x\Delta s}-\frac{2}{\Delta z^2}-\frac{2}{\Delta y^2}\right)\prod_{\xi,l}^{m+1,p,q}\\ &+\frac{1}{\Delta z^2}\prod_{\xi,l}^{m+1,p,q-1}+\frac{1}{\Delta y^2}\prod_{\xi,l}^{m,p+1,q}+\frac{1}{\Delta y^2}\prod_{\xi,l}^{m+1,p+1,q}+\frac{1}{\Delta z^2}\prod_{\xi,l}^{m+1,p,q+1}+\frac{1}{\Delta y^2}\prod_{\xi,l}^{m,p-1,q}+\frac{1}{\Delta z^2}\prod_{\xi,l}^{m,p,q-1}+\left(-\frac{8}{\Delta x\Delta s}-\frac{2}{\Delta z^2}-\frac{2}{\Delta y^2}\right)\prod_{\xi,l}^{m,p,q}\qquad\xi=x,y,z\end{aligned}. \tag{10}$$

By using the CN FD scheme to solve (9), the discrete form of vector TDPE can be derived as (10), where $\Pi_{\xi,l}^{m,p,q}$ represents the reduced transient scattered field at the location of $(m\Delta x, p\Delta y, q\Delta z)$ at the time step of $l\Delta s$. As observed in (10), the unknown on the $(m+1)$th transverse plane at the $(l+1)$th time step can be calculated from the values on the mth transverse plane at the $(l+1)$th time step and those at the l th time step. The computation process of CN FD scheme is shown in Fig. 1. The calculation can be taken plane by plane with marching along the paraxial direction for each time step. As a result, the computational resources reduce because it converts a 3D problem into several 2D problems. As seen in Fig. 2, every plane consists of 4 parts which need to be mesh: 1) the truncation boundary, 2) free space, 3) the scatterer boundary, and 4) the interior of scatterers. In this paper, the perfect matching layers (PML) are employed to truncate transverse plane and the IBC is adopted according to the thin coat of scatterers. It will be introduced in Section III detailedly. In each solution plane, the fields at the boundary grids of scatterers are computed by IBC and the fields at other grids can be obtained by (10), i.e., the CN FD scheme.

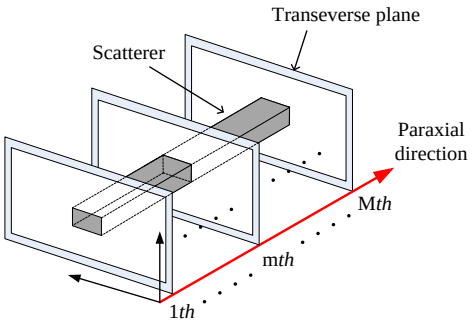

Fig. 1. Computation process of CN FD scheme in TDPE method.

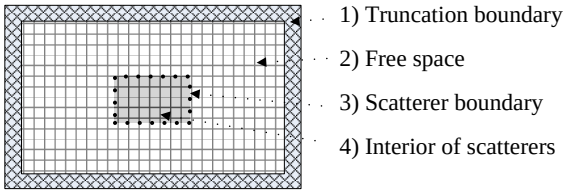

Fig. 2. Computation regions and mesh grids in a transverse plane.

B. Rotating TDPE method

The standard PE gets a good accuracy only in the range of smaller than ±15° around the paraxial direction, as shown in Fig. 3 (a), because the error of first order Taylor series expansion for pseudo differential operator in (4) is proportional to $\sin^4\alpha$, where α is the angle between the observed direction and the paraxial direction. To obtain full-angle scattering fields, the rotating TDPE method is used. In Fig. 3 (b), the paraxial direction is fixed at x-axis while the scatterer and incident wave are rotated by a specified angle to make the observed area around the paraxial direction. After rotation, the grids of targets can be regenerated directly by the coordinate transformation and repartitioned into a new series of transverse planes to be solved. Accordingly, for an irregular and asymmetric target, the full bistatic RCS can be calculated by rotating at least 12 times.

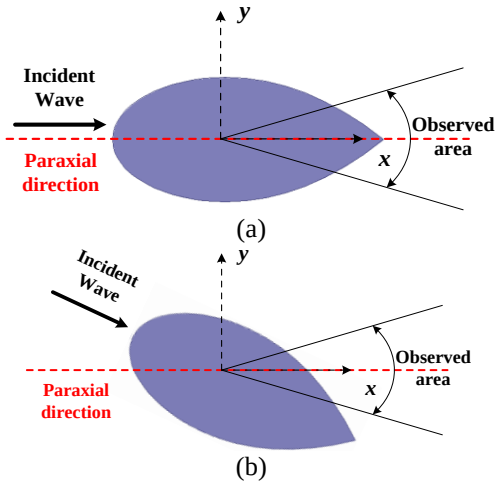

Fig. 3. Scheme of rotating TDPE method. (a) A narrow-anlge scattering pattern around the paraxial direction can be obtained accurately by a single TDPE run. (b) Results of other angles can be obtained by rotating the objects and incident waves.

III. IMPLEMENTATION OF THE TDIBC IN THE TDPE FORMULATION

Leontovich IBC is an approximate boundary condition in the electromagnetic. It constructs a relationship between the the tangential components of the electric field $\boldsymbol{E}$ and the magnetic field $\boldsymbol{H}$. The relation is defined on the outer surface Γ of the thin homogeneous dielectric and the equivalent impedance depends on the coating materials.

Leontovich IBC can be written as follows:

$$\hat{n}\times\mathbf{E}(P) = Z\left[\hat{n}\times\left(\hat{n}\times\mathbf{H}(P)\right)\right], \tag{11}$$

where $\hat{n}$ is the outward directed normal of point P on the Γ. Z represents the surface impedance of point P, which is given by:

$$Z(\omega) = -i\sqrt{\frac{\mu_0\mu_r}{\varepsilon_0\varepsilon_r}}\tan\left(\omega\sqrt{\mu_0\mu_r\varepsilon_0\varepsilon_r}\,d\right), \tag{12}$$

where μ_0, ε_0 is the permeability and permittivity in

free space, μ_r, ε_r is the relative permeability and permittivity of the dielectric and d denotes the thickness of the coating.

As seen from (12), it is difficult to obtain the time-domain expression of Z analytically by using a Fourier transform. Thus we utilize the vector fitting method [28] to solve this problem. $Z(\omega)$ in frequency domain is approximated by the rational fraction in Laplace domain $(s = j\omega)$:

$$Z(s) = \frac{a_0 + a_1 s + \cdots + a_N s^N}{b_0 + b_1 s + \cdots + b_N s^N} . \tag{13}$$

Using partial-fraction expansion, (13) can be rewritten as:

$$Z(s) = c_0 + \sum_{i=1}^{N} \frac{c_i}{s - p_i} , \tag{14}$$

where p_i is the pole and c_i is the residue. In this way, the expression of Z in time domain can be easily obtained:

$$Z(t) = c_0 \delta(t) + \sum_{i=1}^{N} c_i e^{p_i t} . \tag{15}$$

By substituting $\nabla \times \mathbf{E} = iw\mu\mathbf{H}$ to (11), the IBC can be expressed only by electric field $\boldsymbol{E}$:

$$\hat{n} \times \mathbf{E} = \frac{Z}{ikZ_0} \left[\hat{n} \cdot (\nabla \times \mathbf{E}) \hat{n} - \nabla \times \mathbf{E} \right] . \tag{16}$$

It can be transformed into a scalar form:

$$\begin{aligned} &(n_x, n_y, n_z) \times (E_x, E_y, E_z) \\ &= \frac{Z}{ikZ_0} \begin{bmatrix} \left[(n_x, n_y, n_z) \cdot \left(\frac{\partial E_z}{\partial y} - \frac{\partial E_y}{\partial z}, \frac{\partial E_x}{\partial z} - \frac{\partial E_z}{\partial x}, \frac{\partial E_z}{\partial x} - \frac{\partial E_x}{\partial y} \right) \right] (n_x, n_y, n_z) \cdot \\ - \left(\frac{\partial E_z}{\partial y} - \frac{\partial E_y}{\partial z}, \frac{\partial E_x}{\partial z} - \frac{\partial E_z}{\partial x}, \frac{\partial E_z}{\partial x} - \frac{\partial E_x}{\partial y} \right) \end{bmatrix} \end{aligned} \tag{17}$$

The total electric field $\mathbf{E}$ in (16) is the sum of the incident field and scattering field, i.e., $\mathbf{E} = \mathbf{E}^s + \mathbf{E}^i$, where $\mathbf{E}^s = e^{ikx} u$ in PE method. So the scalar form of $\mathbf{E}$ can be written as:

$$(E_x, E_y, E_z) = (E_x^i + e^{ikx} u_x, E_y^i + e^{ikx} u_y, E_x^i + e^{ikx} u_z) . \tag{18}$$

By substituting (20) into (17) and separating the incident field and scattering field, three scalar equations can be derived as:

$$\begin{aligned} &n_y u_z - n_z u_y - \frac{Z}{ikZ_0} \begin{bmatrix} (n_x^2 - 1) \left(\frac{\partial u_z}{\partial y} - \frac{\partial u_y}{\partial z} \right) + n_x n_y \left(\frac{\partial u_x}{\partial z} - \frac{\partial u_z}{\partial x} - iku_z \right) \\ + n_x n_z \left(iku_y + \frac{\partial u_y}{\partial x} - \frac{\partial u_x}{\partial y} \right) \end{bmatrix} , \\ &= (-n_y E_z^i + n_z E_y^i) e^{-ikx} + \frac{Ze^{-ikx}}{ikZ_0} \begin{bmatrix} (n_x^2 - 1) \left(\frac{\partial E_z^i}{\partial y} - \frac{\partial E_y^i}{\partial z} \right) \\ + n_x n_y \left(\frac{\partial E_x^i}{\partial z} - \frac{\partial E_z^i}{\partial x} \right) + n_x n_z \left(\frac{\partial E_y^i}{\partial x} - \frac{\partial E_x^i}{\partial y} \right) \end{bmatrix} \end{aligned} \tag{19}$$

$$\begin{aligned} &n_z u_x - n_x u_z - \frac{Z}{ikZ_0} \begin{bmatrix} n_x n_y \left(\frac{\partial u_z}{\partial y} - \frac{\partial u_y}{\partial z} \right) + (n_y^2 - 1) \left(\frac{\partial u_x}{\partial z} - \frac{\partial u_z}{\partial x} - iku_z \right) \\ + n_y n_z \left(iku_y + \frac{\partial u_y}{\partial x} - \frac{\partial u_x}{\partial y} \right) \end{bmatrix} , \\ &= (-n_z E_x^i + n_x E_z^i) e^{-ikx} + \frac{Ze^{-ikx}}{ikZ_0} \begin{bmatrix} n_x n_y \left(\frac{\partial E_z^i}{\partial y} - \frac{\partial E_y^i}{\partial z} \right) + (n_y^2 - 1) \left(\frac{\partial E_x^i}{\partial z} - \frac{\partial E_z^i}{\partial x} \right) \\ + n_y n_z \left(\frac{\partial E_y^i}{\partial x} - \frac{\partial E_x^i}{\partial y} \right) \end{bmatrix} \end{aligned} \tag{20}$$

$$\begin{aligned} &n_x u_y - n_y u_x - \frac{Z}{ikZ_0} \begin{bmatrix} n_x n_z \left(\frac{\partial u_z}{\partial y} - \frac{\partial u_y}{\partial z} \right) + n_y n_z \left(\frac{\partial u_x}{\partial z} - \frac{\partial u_z}{\partial x} - iku_z \right) \\ + (n_z^2 - 1) \left(iku_y + \frac{\partial u_y}{\partial x} - \frac{\partial u_x}{\partial y} \right) \end{bmatrix} . \\ &= (-n_x E_y^i + n_y E_x^i) e^{-ikx} + \frac{Ze^{-ikx}}{ikZ_0} \begin{bmatrix} n_x n_z \left(\frac{\partial E_z^i}{\partial y} - \frac{\partial E_y^i}{\partial z} \right) + n_y n_z \left(\frac{\partial E_x^i}{\partial z} - \frac{\partial E_z^i}{\partial x} \right) \\ + (n_z^2 - 1) \left(\frac{\partial E_y^i}{\partial x} - \frac{\partial E_x^i}{\partial y} \right) \end{bmatrix} \end{aligned} \tag{21}$$

Therefore, the time-domain IBC can be derived from (19)~(21) by using Fourier transforms. It should be noted that the convolution operation $Z(t) * \prod(t)$ can be expanded by [29]:

$$\begin{aligned} Z(t) * \prod(t)\big|_{t=n\Delta t} &= \left(c_0 \delta(t) + \sum_{i=1}^{N} c_i e^{p_i t} \right) * \prod(t) \Big|_{t=n\Delta t} \\ &= c_0 \prod^{(n)} + \sum_{i=1}^{N} c_i e^{p_i t} * \prod(t) \Big|_{t=n\Delta t} \\ &\approx c_0 \prod^{(n)} + \sum_{i=1}^{N} \left[\chi_i^{(0)} \prod^{(n)} + \sum_{k=1}^{n} \chi_i^{(k)} \prod^{(n-k)} \right] \end{aligned} , \tag{22}$$

where $\chi_i^{(0)} = \int_0^{\Delta t/2} c_i e^{p_i \tau} d\tau$, $\chi_i^{(k)} = \int_{(k-1/2)\Delta t}^{(k+1/2)\Delta t} c_i e^{p_i \tau} d\tau$, n denotes the number of time steps and Δt denotes the time increment.

Let $\psi_i^{(n)} = \sum_{k=1}^{n} \chi_i^{(k)} \prod^{(n-k)}$ and it can be computed by the recursion convolution:

$$\psi_i^{(n)} = -\frac{c_i}{p_i} (1 - e^{p_i \Delta t}) e^{p_i \Delta t / 2} \prod^{(n-1)} + e^{p_i \Delta t} \psi_i^{(n-1)} . \tag{22}$$

By substituting (24) to (23), $Z(t) * \prod(t)$ can be calculated quickly. This approach avoids numerous integral operations in the convolution and saves computational time.

IV. NUMERICAL RESULTS

All the numerical results are tested on Lenovo personal computer of Inter Q9500 (2.83GHz) with RAM of 8G. The incident source for all the examples in this paper is the modulated Gaussian pulse, and it can be written as:

$$\mathbf{E}^{\mathbf{i}} (\boldsymbol{r}, t) = \hat{n} \exp \left(-\frac{(t - \boldsymbol{r} \cdot \hat{k}/c - \tau_p)^2}{2\sigma^2} \right) , \tag{23}$$

where $\hat{n}$ is the unit vector of electrical field, $\hat{k}$ is the wave vector, $\tau_p = 10\sigma$ is the time delay, $\sigma = 3/(\pi f_{bw})$ is the pulse width and f_{bw} is the bandwidth.

A. Wide-band scattering from a coated PEC cylinder

We firstly analyze a coated PEC cylinder with radius of 2*m* and height of 2*m* by using the proposed method and the time domain integral equation (TDIE) method with IBC, which is computed by in-house code. The relative complex permittivity of the coating material is $\varepsilon_r = \varepsilon' - \mathrm{j}\varepsilon'' = 2 - \mathrm{j}$ and the relative permeability is $\mu_r = 1$. The thickness of coating material is 0.01m. As shown in the inset of Fig. 4, a *y*-polarization plane wave illuminates along the center axis of the cylinder. Both the incident direction and paraxial direction of TDPE method are along the +*x* axis. The bandwidth of the modulated Gaussian pulse in this example is 600MHz. The bistatic RCS calculated by TDIE and TDPE at 200MHz, 300MHz and 400MHz are shown in Figs. 4 (a)-(c). It can be found that there is a good agreement between them. The bistatic RCS for all azimuthal angles is obtained by rotating TDPE. In order to evaluate the error in the TDPE method, the root mean square errors (RMSE) of RCS changing with the azimuthal angle φ are defined as:

$$\mathrm{RMSE} = \sqrt{\frac{1}{N}\sum_{i=1}^{N}\left|\sigma_i - \sigma_i^{IE}\right|^2}, \qquad (24)$$

where N is the number of frequency points, σ_i and σ_i^{IE} are the RCS values computed by TDPE and TDIE with IBC at the i th frequency point, respectively. Figure 5 compares the errors of RCS ranging from $\varphi = 0°$ to 45° which are obtained by a single TDPE run and rotating TDPE method. It can be observed that the RMSE of a single TDPE run stays lower than 1dB within 15° along the paraxial direction and increases as angle becomes larger. It proves the fact that the standard TDPE only gets a good accuracy only within a narrow-angle range around the paraxial direction and the full bistatic RCS can be obtained by using rotating TDPE method, as described in Section II. In this example, 7 rotating TDPE runs are used to obtain the final results. Figure 6 gives the comparison between the two methods on the magnitudes of reduced transient scattered fields at the point of (2*m*, 2.6*m*, 0*m*). It also verifies the accuracy of the proposed method and the late-time behavior is stable because of the CN FD scheme. To discuss the influence of dielectric loss on the proposed method, three different kinds of coated materials with $\varepsilon_r = 2 - 0.1\mathrm{j}$, $\varepsilon_r = 2 - 0.5\mathrm{j}$ and $\varepsilon_r = 2 - 1.0\mathrm{j}$ are analyzed and compared. Table 1 shows the average RMSE with respect to the TDIE results, defined as $\sum_{i=1}^{M}\mathrm{RMSE}/M$ (M is the number of calculated angles). It can be seen that the errors for all three materials achieve a low level lower than 1dB and are almost independent of frequencies. The proposed method has a high accuracy when the thickness of coated material is small.

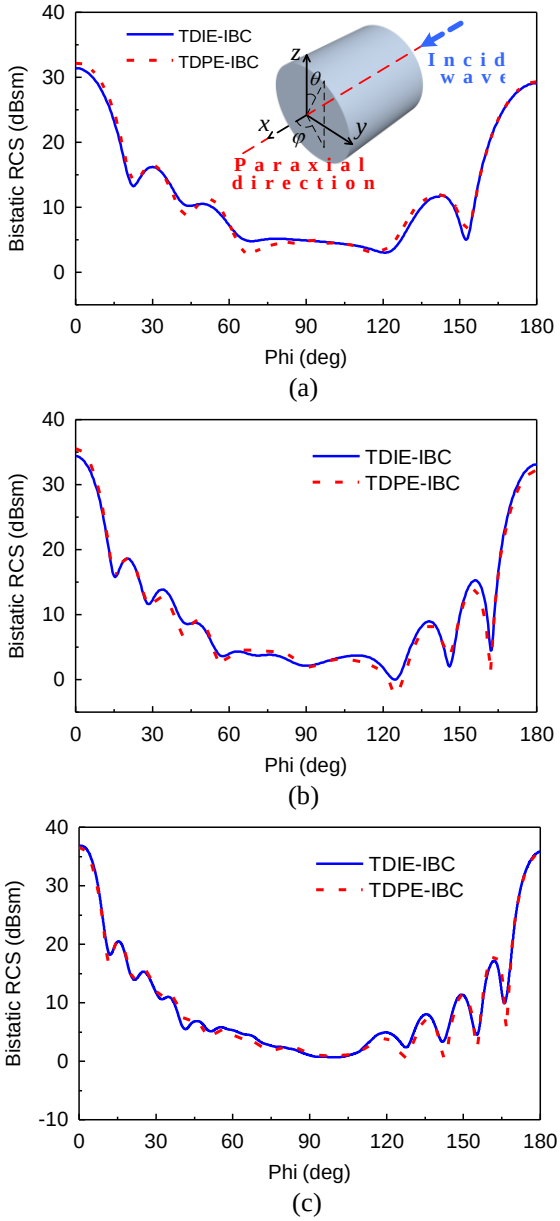

Fig. 4. Bistatic RCS of a coated PEC cylinder at different frequencies: (a) f = 200 MHz, (b) f = 300 MHz, and (c) f = 400 MHz. The incident direction of the plane wave is shown in the inset of (a).

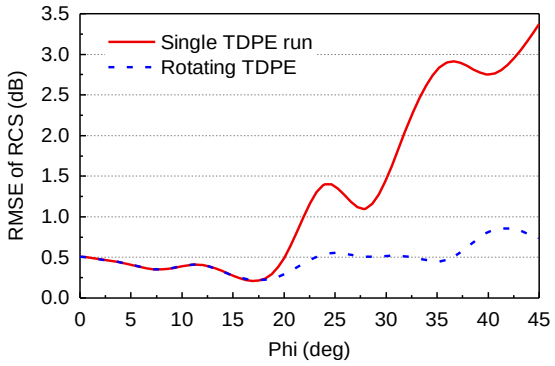

Fig. 5. Comparison of RMSE for bistatic RCS calculated by a single TDPE run and the rotating TDPE method.

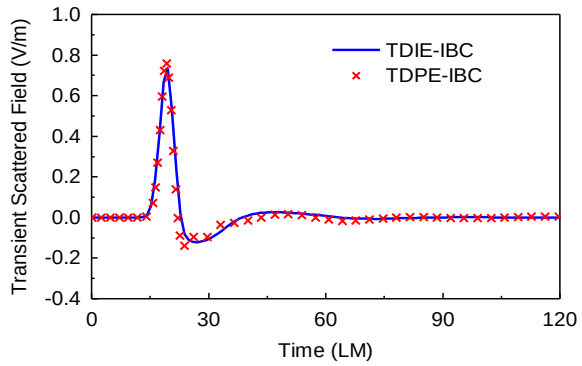

Fig. 6. Transient scattered field at the point (2*m*, 2.6*m*, 0*m*). The unit LM represents light meter and 1LM = 1/c, where c is the light speed in free space.

Table 1: Average RMSE calculated for different coated materials with different permittivity

Material Constant	Average RMSE(dB)
$\varepsilon_r = 2 - 0.1\mathrm{j}$	0.60
$\varepsilon_r = 2 - 0.5\mathrm{j}$	0.61
$\varepsilon_r = 2 - 1.0\mathrm{j}$	0.58

B. Wide-band scattering from a coated PEC spherical cone

To discuss the accuracy and efficiency of the proposed method further, the broadband scattering of a coated PEC spherical cone is analyzed. The cone is coated with dielectric of $\varepsilon_r = 2 - \mathrm{j}$, $\mu_r = 1$ and the thickness is 0.01m. The radius of the hemisphere is 4m and the height of the cone is 6m. The simulated scenario is shown in the inset of Fig. 7. A *y*-polarization plane wave illuminates from the top of the cone. Both the incident direction and paraxial direction of TDPE method are also along the +*x* axis. The bandwidth of the modulated Gaussian pulse in this example is 1GHz. The full bistatic RCS results computed by rotating TDPE at 200MHz, 500MHz and 800MHz achieve a good agreement with the results of TDIE in Figs. 7 (a)-(c). This demonstrates that the proposed method is still accurate when the frequency band is further broadened. The transient forward-scattered field values are presented in Fig. 8, where a remarkable consistence is achieved between the two methods. Additionally, the computational resources of the two methods are compared in Table 2. It can be found that both the memory requirement and the time consumption reduce significantly for the proposed method. Therefore, it is an efficient tool to analyze the wideband scattering from electrically large coated objects.

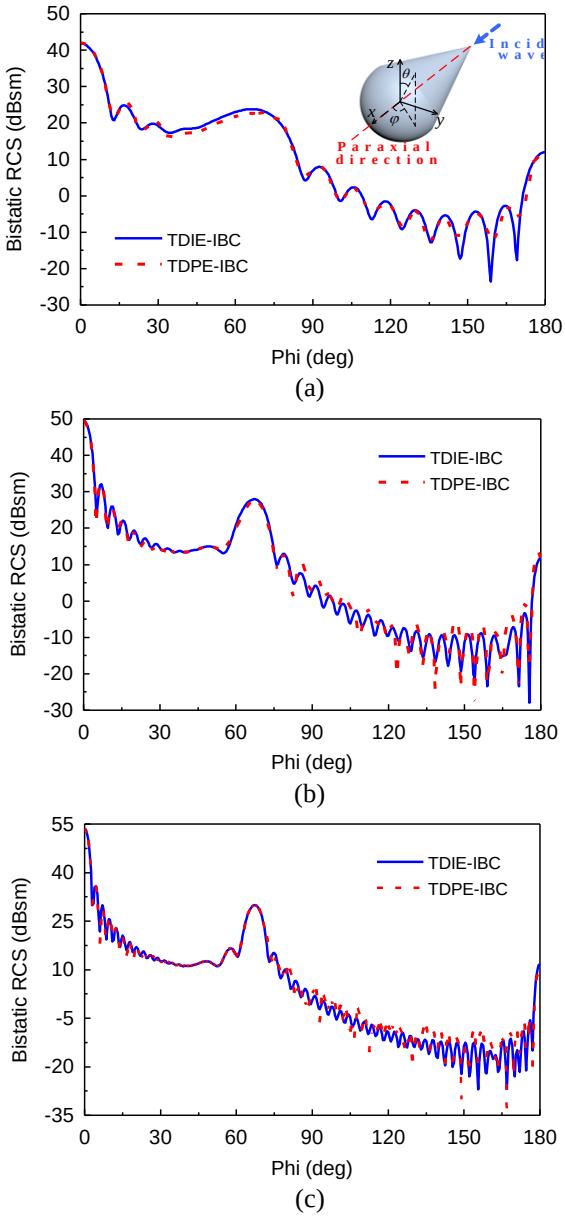

Fig. 7. Bistatic RCS of a coated PEC spherical cone at different frequencies: (a) f = 200 MHz, (b) f = 500 MHz, and (c) f = 800 MHz. The incident direction of the plane wave is shown in the inset of (a).

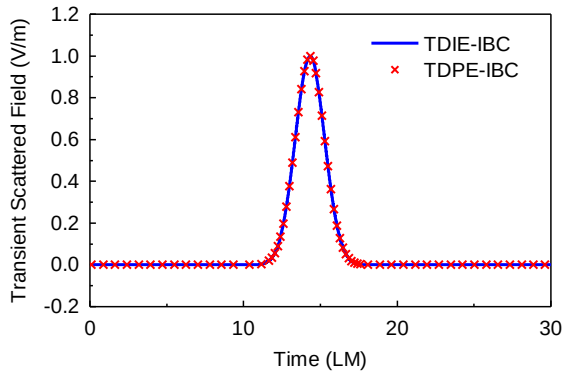

Fig. 8. Transient scattered field at the point (10*m*, 2*m*, 0*m*). The unit LM represents light meter and 1LM = 1/c, where c is the light speed in free space.

Table 2: Comparison of the computational resources for the TDIE with IBC method and the proposed method

Methods	Peak Memory Requirement (MB)	Total CPU Time (h)
TDIE-IBC	8562	18.9
TDPE-IBC	352	10.8

VI. CONCLUSION

In this paper, we propose the time-domain parabolic equation method with impedance boundary condition to analyze the wideband scattering from electrically large coated objects. The TDPE method increases the efficiency by converting the three-dimensional problem to multiple two-dimensional problems. And additionally, most of the computational resources do not need to be consumed on the dielectric regions due to the impedance boundary condition. The accurate bistatic RCS for all directions can be obtained by the rotating TDPE method. Numerical results have validated the accuracy and efficiency of this method.

ACKNOWLEDGMENT

This work was supported by the Natural Science Foundation under Grant 61701240, Fundamental Research Funds for the Central Universities with No. 30918011317, and State Key Laboratory of Millimeter Waves under Grant K201920.

REFERENCES

[1] A. C. Rappaport, "On the parabolic equation method for water-wave propagation," *J. Fluid. Mech.*, vol. 95, no. 1, pp. 159-176, 1979.

[2] R. A. Dalrymple and P. A. Martin, "Perfect boundary conditions for parabolic water-wave models," *Proc. R. Soc. London A*, vol. 437, pp. 41-54, 1992.

[3] M. D. Feit and J. A. Fleck, Jr., "Light propagation in graded-index fibers," *Appl. Opt.*, vol. 17, pp. 3990-3998, 1978.

[4] D. Yevick, "A guide to electric field propagation techniques for guided-wave optics," *Opt. Quantum Electron.*, vol. 26, pp. 185-197, 1994.

[5] F. Collino and P. Joly, "Splitting of operators, alternate directions, and paraxial approximations for the three-dimensional wave equation," *SIAM J. Sci. Comput.*, vol. 16, pp. 1019-1048, 1995.

[6] M. Leontovich and V. Fock, "Solution of the problem of propagation of electromagnetic waves along the earth's surface by the method of parabolic equation," *Acad. Sci. Ussr. J. Phys.*, vol. 7, pp. 557-573, 1946.

[7] Q. F. Wei, C. Y. Yin, and W. Wu, "Research and verification for an improved two-way parabolic equation method in obstacle environment," *IET Microwaves, Antennas & Propag.*, vol. 12, no. 4, pp. 576-582, 2018.

[8] M. F. Levy, "Parabolic equation modeling of propagation over irregular terrain," *Electron. Lett.*, vol. 26, pp. 1153-1155, 1990.

[9] Z. He, H. Zeng, and R. S. Chen, "Two way propagation modeling of expressway with vehicles by using the three-dimensional ADI-PE method," *IEEE Trans. Antennas Propag.*, vol. 66, no. 4, pp. 2156-2160, Apr. 2018.

[10] Z. He, Z. H. Fan, D. Z. Ding, and R. S. Chen, "Efficient radar cross-section computation of electrically large targets with ADI-PE method," *Electron. Lett.*, vol. 51, no. 4, pp. 360-362, 2015.

[11] Z. He and R. S. Chen, "A vector meshless parabolic equation method for three-dimensional electromagnetic scatterings," *IEEE Trans. Antennas Propag.*, vol. 63, no. 6, pp. 2595-2603. 2015.

[12] Z. He and R. S. Chen, "A novel parallel parabolic equation method for electromagnetic scatterings," *IEEE Trans. Antennas Propag.*, vol. 64, no. 11, pp. 4777-4784, 2016.

[13] Z. He, Z. H. Fan, D. Z. Ding, and R. S. Chen, "GPU-accelerated ADI-PE method for the analysis of EM scatterings," *Electron. Lett.*, vol. 51, pp. 1652-1654, 2015.

[14] Z. He and R. S. Chen, "A novel marching-on-in-degree solver of time domain parabolic equation for transient EM scattering analysis," *IEEE Trans. Antennas Propag.*, vol. 61, no. 11, pp. 4905-4910, 2016.

[15] Z. He and R. S. Chen, "Frequency-domain and time-domain solvers of parabolic equation for rotationally symmetric geometries," *Comput. Phys. Commun.*, vol. 220, pp. 181-187, 2017.

[16] J. E. Murphy, "Finite-difference treatment of a time-domain parabolic equation: Theory," *J. Acoust. Soc. Am.*, vol. 77 no. 5 pp. 1958-1960, 1985.

[17] Z. He, R. S. Chen, "Fast analysis of wide-band scattering from electrically large targets with

time-domain parabolic equation method," *Comput. Phys. Commun.*, vol. 200, pp. 139-146, 2016.

[18] Z. He, D. Z. Ding, and R. S. Chen, "An efficient marching-on-in-degree solver of surface integral equation for multilayer thin medium-coated conductors," *IEEE Antennas & Wireless Propag. Lett.*, vol. 15, pp. 1458-1461, 2016.

[19] Z. He and R. S. Chen, "A fast marching-on-in-degree solution for analysis of conductors coated with thin dispersive dielectric," *IEEE Trans. Antennas Propag.*, vol. 65, no. 9, pp. 4751-4758, 2017.

[20] Z. He, Z. H. Fan, D. Z. Ding, and R. S. Chen, "Solution of PMCHW integral equation for transient electromagnetic scattering from dielectric body of revolution," *IEEE Trans. Antennas Propag.*, vol. 63, no. 11, pp. 5124-5129, 2015.

[21] Z. He, R. S. Chen, and W. Sha, "An efficient marching-on-in-degree solution of transient multi-scale EM scattering problems," *IEEE Trans. Antennas Propag.*, vol. 64, no. 7, pp. 3039-3046, 2016.

[22] Z. H. Fan, Z. He, and R. S. Chen, "Marching-on-in-degree solution of the transient scattering from multiple bodies of revolution," *IEEE Trans. Antennas Propag.*, vol. 64, no. 1, pp. 321-326, 2015.

[23] Z. He and R. S. Chen, "An efficient high-order marching-on-in-degree solver for conducting and dielectric bodies of revolution," *Trans. Antennas Propag*, vol. 65, no. 8, pp. 4374-4378, 2017.

[24] Z. He, H. H. Zhang, and R. S. Chen, "Parallel marching-on-in-degree solver of time-domain combined field integral equation for bodies of revolution accelerated by MLACA," *IEEE Trans. Antennas Propag.*, vol. 63, no. 8, pp. 3705-3710, 2015.

[25] T. K. Sarkar and E. Arvas, "An integral equation approach to the analysis of finite microstrip antennas: Volume/surface formulation," *IEEE Trans. Antennas Propag.*, vol. 38, no. 3, pp. 305-312, Mar. 1990.

[26] T. B. A. Senior, "Impedance boundary conditions for imperfectly conducting surfaces," *Appl. Sci. Res.*, vol. 8, no. 1, pp. 418, 1960.

[27] Q. Chen, M. Lu, and E. Michielssen, "Integral equation based analysis of transient scattering from surfaces with impedance boundary condition," *IEEE Antennas and Propag. Society Symp., 2004*, Monterey, CA, USA, vol., 4, pp. 3891-3894, 2004.

[28] B. Gustavsen and A. Semlyen, "Rational approximation of frequency domain responses by vector fitting," *IEEE Trans. Power Delivery*, vol. 14, no. 3, pp. 1052-1061, 1999.

[29] J. M. Jin, *The Finite Element Method in Electromagnetics*. *John Wiley & Sons*, 2015.

Ling Guan was born in Nanjing, China. He received the B.S. degree in Communication Engineering from the School of Electrical Engineering and Optical Technique, Nanjing University of Science and Technology, Nanjing, China, in 2014. He is currently pursuing his Ph.D. degree in Electronic Engineering at Nanjing University of Science and Technology.

His research interests are antennas, metamaterials and computational electromagnetics.

Shifei Tao was born in Anhui, China, in 1987. He received the B.Sc. degree in Communication Engineering and Ph.D. degree in EM Field and Microwave Technique from Nanjing University of Science and Technology (NJUST), Nanjing, Jiangsu, China, in 2008 and 2014, respectively.

Since 2017, he has been with Nanjing University of Science and Technology, where he works as an Assistant Professor. From 2015 to 2016, he was a Postdoctoral Research Associate in Electric and Computer Engineering in Northeastern University, Boston, USA. His current research interests are in the computational electromagnetics, antennas, electromagnetic scattering and radiation.